Check for updates

Received: 23 March 2024 | Accepted: 29 July 2024

DOI: 10.1111/imm.13849

ORIGINAL ARTICLE

immunology
Insights into immunity in health and disease

Mast cells contribute to T-cell accumulation in the bronchoalveolar space in mice with IL-33-induced airway inflammation

P. Abigail Alvarado-Vazquez | **Erika Mendez-Enriquez** | **Lisa Pähn** | **Aleksandra Dondalska** | **Diego Pazos-Castro** | **Jenny Hallgren**

Department of Medical Biochemistry and Microbiology, Uppsala University, Uppsala, Sweden

Correspondence
P. Abigail Alvarado-Vazquez and Jenny Hallgren, Department of Medical Biochemistry and Microbiology, Uppsala University, 751 23 Uppsala, Sweden.
Email: palvaradovazquez@health.ucsd.edu and jenny.hallgren@imbim.uu.se

Present address
P. Abigail Alvarado-Vazquez, Department of Medicine, University of California, San Diego, La Jolla, California, USA.

Funding information
Vetenskapsrådet, Grant/Award Number: 2016- 00803; 2023-01848; Cancerfonden, Grant/Award Number: 22 21 15; Knut och Alice Wallenbergs Stiftelse, Grant/Award Number: 2017.0022; Ruth and Nils-Erik Stenbäcks Stiftelse; Konsul Th C Berghs Stiftelse; Hans von Kantzows Stiftelse

Abstract

Interleukin (IL)-33 released from airway epithelial cells plays a vital role in shaping type 2 immune responses by binding to the ST2 receptor present in many immune cells, including mast cells (MCs). Intranasal administration of IL-33 in mice induces type 2 lung inflammation, an increase in lung MC progenitors, and transepithelial migration of leukocytes to the bronchoalveolar space. The aim of this study was to determine the contribution of MCs in IL-33-induced lung pathology. Four daily intranasal administrations of IL-33 reduced spirometry-like lung function parameters, induced airway hyperresponsiveness, and increased leukocytes in bronchoalveolar lavage fluid (BAL) in an ST2-dependent manner. MC-deficient ($Cpa3^{cre/+}$) mice, which lack MCs, had intact spirometry-like lung function but slightly reduced airway hyperresponsiveness, possibly related to reduced IL-33 or serotonin. Strikingly, $Cpa3^{cre/+}$ mice exposed to IL-33 had 50% reduction in BAL T-cells, and CXCL1 and IL-33 were reduced in the lung. Intranasal IL-33 induced CXCR2 expression in T-cells in a MC-independent fashion. Furthermore, IL-33-induced lung MCs were immunopositive for CXCL1 and localized in the epithelium of wild-type mice. These results suggest that MCs are required to sustain intact lung IL-33 and CXCL1 levels in mice with IL-33-induced airway inflammation, thereby facilitating T-cell accumulation in the bronchoalveolar space.

KEYWORDS
CXCL1, CXCR2, IL-33, lung, mast cells, T-cells

INTRODUCTION

The alarmin interleukin (IL)-33 is released from the lung epithelium in response to cellular stresses such as microbes, allergens, and other environmental cues. IL-33 acts via its receptor ST2, and the IL-1 receptor accessory protein to regulate the survival, proliferation, and

Abbreviations: 5-HT, serotonin; AHR, airway hyperresponsiveness; BAL, bronchoalveolar lavage fluid; FEV 0.1, forced expired volume in 0.1 s; FVC, forced vital capacity; IC, inspiratory capacity; MCs, mast cells; mMCP, mouse MC protease; PEF, peak of expiratory flow.

This is an open access article under the terms of the Creative Commons Attribution License, which permits use, distribution and reproduction in any medium, provided the original work is properly cited.
© 2024 The Author(s). *Immunology* published by John Wiley & Sons Ltd.

function of ST2-bearing immune cells including innate lymphoid cells type 2 (ILC2s) and mast cells (MCs) [1]. IL-33 also activates ST2-expressing memory T helper 2 (Th2)-cells to produce IL-13 and IL-5 [2], and FoxP3$^+$ T-regulatory cells (T-regs) to produce tissue repair-promoting amphiregulin [3].

The IL-33/ST2 axis has been linked to asthma in multiple studies. For example, the genes coding for IL-33 and ST2 are loci associated to asthma susceptibility [4]. Moreover, increased levels of IL-33 are found in serum and bronchoalveolar lavage fluid (BAL) from asthma patients and correlate with reduced lung function [5, 6]. In patients with allergic asthma, MCs accumulate at specific sites of the lung such as in the epithelium and the smooth muscle [7, 8]. Similarly in mice, antigen exposure via the airways increases the lung MC compartment at the similar sites due to the recruitment and expansion of MC progenitors originating in the bone marrow [9–12].

To our knowledge, MCs from different tissues and developmental stages consistently exhibit ST2 surface expression. IL-33 induces cytokine-release from MCs [13, 14], and potentiates IgE-mediated release of proinflammatory mediators [15]. Additionally, MCs can also be a source of IL-33 [16]. To determine the specific role of IL-33 in airway diseases, several studies have used intranasal administrations of IL-33 in mice to induce antigen-independent airway inflammation. These studies have demonstrated the induction of airway hyperresponsiveness (AHR) independent of adaptive immunity, but dependent on IL-13 at least partly produced by ILC2s [17, 18]. Since we previously showed that intranasal administration of IL-33 in mice causes an ST2-dependent increase in lung MC progenitors [19] and that lung MC progenitors can produce IL-13 [20], we hypothesized that MCs are involved in mediating the type 2 lung pathology induced by intranasal IL-33 in mice. In the current study, we show that MCs contribute to IL-33-induced airway inflammation by promoting production of IL-33 and CXCL1 in the lungs, thereby facilitating the accumulation of CXCR2$^+$ T-cells in the bronchoalveolar space.

METHODS

Mice

All experiments were approved and performed in accordance with the Uppsala animal ethics committee (5.8.18-05248/2018; 5.8.18-21870/2022). All mice were bred and housed at the National Veterinary Institute (Uppsala, Sweden). The BALB/c mice were from Taconic (BALB/c BomTac), and bred with ST2$^{-/-}$ and Cpa3$^{cre/+}$ mice to generate littermate controls. Cpa3$^{cre/+}$ [21] and Il1rl1 (ST2)$^{-/-}$ [22] mice were originally provided by Hans-Reimer Rodewald and Andrew McKenzie, respectively.

Model of IL-33-induced airway inflammation

Mature mouse IL-33 (Peprotech) or vehicle (0.1% of bovine serum albumin in PBS) was administrated intranasally in 20 µL per nostril for four consecutive days to anaesthetised mice (1% isoflurane). A dose of 3 µg/mouse/day was used for all experiments except for the assessment of AHR when 1 µg/mouse/day was used to avoid hyper mucus secretion in response to methacholine.

Model of HDM-induced airway inflammation

House dust mite extract (HDM) from the European HDM species *Dermatophagoides pteronyssius* was purchased from Stallargenes Greer. The extract was reconstituted in sterile 1× PBS and kept at −80°C. Anaesthetised mice (1% isoflurane) received 50 µg/mouse intranasally in 20 µL per nostril for four times on days 0, 3, 6, and 9. Samples were collected at day 10.

Lung function tests

Mice were anaesthetised using 100 mg/kg ketamine (Pfizer), 20 mg/kg xylazine (Bayer), and 3 mg/kg acepromazine (Pharmaxin) intraperitoneally. Spirometry-like parameters using the Buxco PFT system (Data Sciences International; DSI). Anaesthetised mice were connected to the Buxco PFT system via the trachea and ventilated at 150 breaths per minute. The system is controlled by the FinePointe software, which utilizes the Boyle's Law, quasistatic pressure–volume curves, and fast-volume manoeuvres to calculate peak of expiratory flow (PEF), forced expired volume in 100 ms (FEV 0.1), forced vital capacity (FVC), and inspiratory capacity (IC) parameters. To analyse AHR, anaesthetised mice were connected to a Buxco Fine Point RC system (DSI) through the trachea, and after equilibration was reached, the airways were consecutively exposed to PBS, 5, 10, and 20 mg/kg of aerosolized methacholine to measure airway resistance.

13652567, 2024, 3, Downloaded from https://onlinelibrary.wiley.com/doi/10.1111/imm.13849 by Uppsala University Library, Wiley Online Library on [18/02/2025]. See the Terms and Conditions (https://onlinelibrary.wiley.com/terms-and-conditions) on Wiley Online Library for rules of use; OA articles are governed by the applicable Creative Commons License

Isolation of BAL and lung cells

Mice were euthanized by isoflurane overdose. BAL was obtained by rinsing the airways with 1 mL of 1× PBS. The fluid was centrifuged at 400 g × 5 min, and the supernatant removed and stored at −80°C until analysis. The pellet was treated with ACK solution (150 mM NH_4Cl, 9.5 mM $NaHCO_3$, 1.2 mM EDTA) to lyse red blood cells and washed once with fluorescence activated cell sorting (FACS) buffer (2% heat-inactivated fetal calf serum in 1× PBS). To isolate lung cells, the lungs from euthanized mice were perfused with 10 mL of cold PBS to remove the blood. The lungs were carefully dissected, cut into small pieces, and a single-cell suspension was generated by enzymatic digestion (Lung Dissociation Kit for mouse, Miltenyi Biotec) using the gentleMACS™ Octo Dissociator (Miltenyi). The remaining enzymes were removed by washing once with FACS buffer for 5 min at 400 × g. The samples were resuspended in 10 mL of 44% percoll (Sigma-Aldrich) and centrifuged for 20 min at 400 g to remove epithelial cells and cell debris. The cell pellet was treated with ACK solution for 1 min to remove the remaining red blood cells. Live BAL and lung cells were counted using a haemocytometer chamber and trypan blue exclusion test. In some experiments, the BAL cells were resuspended in PBS, and cytocentrifugated (Shandon) onto microscope slides (Thermo Scientific). The slides were allowed to dry before Diff-quick staining (cat# 2115; Labex AB) to visualize the BAL cells.

Flow cytometry

BAL and lung cell suspensions were passed through a 70 μm strainer before staining for 30 min with the antibodies listed in Table S1. For the extracellular detection of CXCR2, the cells were incubated at 37°C, otherwise the cells were incubated with the antibodies at 4°C. The staining of intracellular markers such as FoxP3 and GATA-3 was performed in fixed lung cells using the fixation/permeabilization buffer set (eBioscience). Gating was set using fluorophore-matched isotype controls. The flow cytometry was performed on Fortessa flow cytometer (BD Biosciences), and data analysis was performed using FlowJo software (BD Biosciences).

Cytokine array

Lungs were collected from PBS-perfused euthanized mice 30 min after the last IL-33 administration and placed in 900 μL of 1× PBS containing protease inhibitor cocktail (Thermo Fisher). Lung lysates were prepared using a tissue homogenizer (polytron PT1200, Kinematica AG) and frozen at −80°C until analysis. After thawing, the samples were centrifugated at 10 000 g for 10 min to remove cellular debris, and the protein concentration determined using Bradford protein assay (Sigma-Aldrich). A total of 300 μg protein/membrane were used in the proteome profiler cytokine array (R&D systems cat#ARY006) following the manufacturer's instructions. The nitrocellulose membranes were incubated with the lung homogenates overnight at 4°C, washed and developed using the reagents provided by the kit. The chemiluminescence was developed in a Chemi-Doc MP imaging system (Bio-Rad), and the densitometry analysis was performed in Fiji by normalizing the expression of each cytokine against the mean of the $Cpa3^{+/+}$ group.

Histology and confocal microscopy

PBS-perfused lungs of euthanized mice were filled with 1 mL of optimal cutting compound (OCT; VWR), placed in 4% formaldehyde in PBS for 24 h, and cryoprotected by incubation in a 20% sucrose in PBS solution for at least 3 days. The left lobe of the lung was embedded in an OCT block and sliced at 20 μm thickness in a cryostat (Thermo Fisher). The sections were blocked and permeabilized with 1% protein-free blocking buffer (Pierce solution, Thermo Fisher) containing 3% triton-X 100 (Sigma-Aldrich) for 1 h at room temperature. Slides were incubated with a primary antibody against mouse CXCL1 (goat anti-mouse 1:100, R&D cat# MAB3736) and mMCP-6 (rat anti-mouse 1:2000, R&D cat#AF-453) or mMCP-8 (rat anti-mouse 1:100, BioLegend cat#647401), or mouse IL-33 (goat anti-mouse 1:75, R&D cat#AF3626), and integrin β7 (rat anti-mouse 1:20, APC conjugated from BD bioscience cat#551082) overnight at 4°C. Next day, the slides were washed and incubated 2 h with Alexa 647 or Alexa 488 donkey anti-goat and Alexa 488 donkey anti-rat (Thermo Fisher) secondary antibodies. Nuclei were stained with 4′,6-diamidino-2-phenylindole (DAPI; 1:20000; Thermo Fisher), mounted with Fluromont-G (Thermo Fisher), and images obtained using a confocal Zeiss LSM700 microscope.

Quantification of CXCL1, IL-13, IL-33, mMCP-1, and 5-HT

The levels of CXCL1 (R&D cat#DY453), IL-13 (Cat# 88–7137-88), IL-33 (Thermo Fisher Cat# 88–7333-88), and mMCP-1 (Cat# 88–7503-88) were investigated in BAL and lung samples using a sandwich enzyme linked

13652567, 2024, 3, Downloaded from https://onlinelibrary.wiley.com/doi/10.1111/imm.13849 by Uppsala University Library, Wiley Online Library on [18/02/2025]. See the Terms and Conditions (https://onlinelibrary.wiley.com/terms-and-conditions) on Wiley Online Library for rules of use; OA articles are governed by the applicable Creative Commons License

immunology
Insights into immunity in health and disease

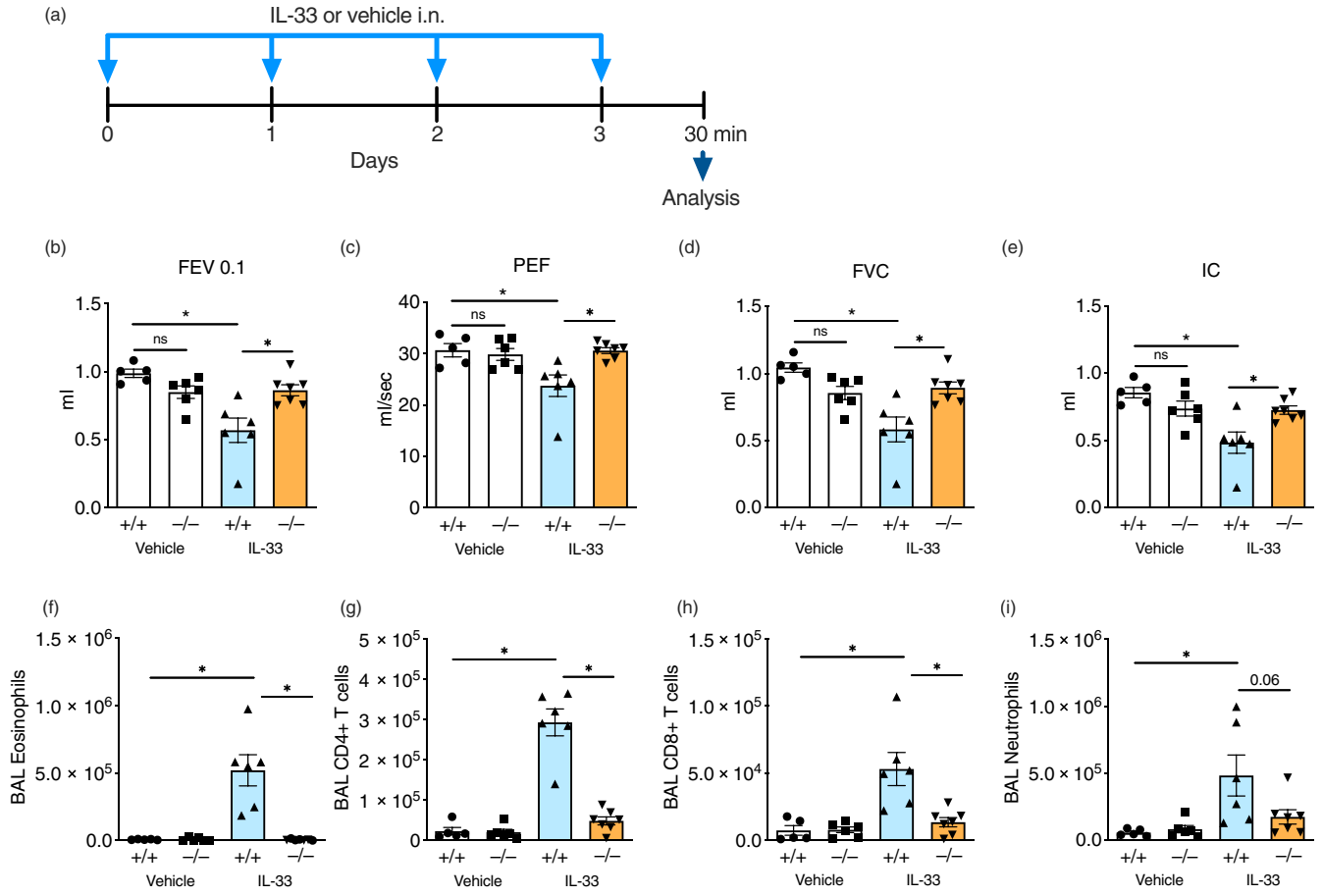

FIGURE 1 Intranasal IL-33 induces reduced lung function and increases BAL cells in a ST2-dependent manner. (a) IL-33 or vehicle (0.1% bovine serum albumin in PBS) was given intranasally daily for four consecutive days and analysed 30 min after the last treatment. (b–e) The spirometry-like parameters forced expired volume in 0.1 s (FEV 0.1) (b), peak of expiratory flow (PEF) (C), forced vital capacity (FVC) (D), and inspiratory capacity (IC) (E) were analysed in ST2 deficient (−/−) and their wild-type littermates (+/+) given IL-33 or vehicle. (f–i) bronchoalveolar lavage fluid (BAL) was collected and analysed by flow cytometry to quantify the number of BAL eosinophils (f), $CD4^+$ (g) and $CD8^+$ T-cells (h), and neutrophils (i). Bars represent mean ± SEM from three pooled independent experiments. Each symbol represents data from an individual mouse. Statistical difference was tested by one-way ANOVA with Tukey post hoc test. Only relevant comparisons are shown (b–i). *$p < 0.05$; ns, no significant difference.

immunosorbent assay (ELISA) kit (Thermo Fisher). The levels of 5-HT were quantified in BAL using a competitive ELISA method (serotonin research ELISA #BA E-5900, LDN). Values outside the detection limit were removed from the analysis.

Statistical analysis

Statistical analysis was performed using GraphPad Prism V.8 (GraphPad software Inc., San Diego, CA). A *p*-value below 0.05 was considered significant. Paired or unpaired Student's *t*-test was used to compare two groups. One-way ANOVA with Bonferroni's post hoc test or two-way ANOVA with repeated measurements was performed when comparing three or more groups.

RESULTS

IL-33 promotes a ST2-dependent decrease in spirometry-like lung function parameters

In a previous study, we established that spirometry-like measurements could be used to monitor HDM-induced allergic airway inflammation in mice [23]. To test whether IL-33 alone can induce changes in spirometry-like lung function, mice received intranasal IL-33 or vehicle daily for four consecutive days, and were analysed 30 min after the last treatment (Figure 1a). IL-33 reduced the forced expiratory volume in 0.1 s (FEV 0.1), peak expiratory flow (PEF), forced vital capacity (FVC), and inspiratory capacity (IC) compared to vehicle controls

13652567, 2024, 3, Downloaded from https://onlinelibrary.wiley.com/doi/10.1111/imm.13849 by Uppsala University Library, Wiley Online Library on [18/02/2025]. See the Terms and Conditions (https://onlinelibrary.wiley.com/terms-and-conditions) on Wiley Online Library for rules of use; OA articles are governed by the applicable Creative Commons License

(Figure S1a–d). However, IL-33 was unable to reduce these parameters in ST2$^{-/-}$ mice (Figure 1b–e). As previously reported [17], IL-33 induced BAL eosinophilia and AHR in response to methacholine (Figure S1e,f). The IL-33-induced increase in BAL eosinophils, CD4^{+} and CD8^{+} T-cells was absent in ST2$^{-/-}$ mice (Figures 1f–h and S1g), and these mice showed a trend ($p = 0.052$) to have reduced levels of neutrophils (Figure 1i). Altogether, IL-33-induced airway inflammation and reduced lung function are mainly mediated by ST2-expressing cells.

IL-33-treated MC-deficient Cpa3$^{cre/+}$ mice have intact spirometry-like lung function parameters but reduced AHR

To test whether MCs contribute to the IL-33-induced lung pathology, we used the Cpa3$^{cre/+}$ mice, which lack MCs due to genotoxic expression of Cre-recombinase under the promotor for the carboxypeptidase A3 (CPA3) gene [21]. As shown [19], intranasal IL-33 induced a 10-fold increase in MC progenitors, identified as CD45^{+} lineage (Lin)$^{-}$ c-kit^{+} FcεRI^{+} CD11b^{-} ST2^{+} Integrin β7^{+} cells, in wild-type (Cpa3$^{+/+}$) littermates compared to vehicle-treated mice (Figures 2a and S2a; Table S1). IL-33-induced lung MC progenitors, which can be identified by their immunopositivity for both the mouse MC protease (mMCP)-6 and integrin β7, localized near the airway epithelium in Cpa3$^{+/+}$ mice (Figure 2k). Flow cytometry revealed that IL-33-treated wild-type littermates had 3 times more MC progenitors than MC-deficient (Cpa3$^{cre/+}$) mice treated in parallel (Figure 2a). Mature MCs were only detected in Cpa3$^{+/+}$ wild-type mice, and their numbers were not increased by the intranasal IL-33 when assessed on day 3 (Figure 2b). Lung basophils, quantified as CD45^{+} Lin^{-} c-kit^{-} FcεRI^{+} CD49b^{+} cells (Figure S2b), were increased in IL-33-treated Cpa3$^{+/+}$ but not in Cpa3$^{cre/+}$ mice (Figure 2c). This could either be explained by Cre-mediated deletion of basophils due to Cpa3 expression in basophil progenitors or that the influx of basophils to the lung is affected by the loss of MCs, or both. The mucosal MC-specific protease, mMCP-1, was increased in BAL from IL-33-treated Cpa3$^{+/+}$ mice compared to vehicle control mice and remained barely detectable in Cpa3$^{cre/+}$ mice treated in parallel (Figure 2d). In summary, IL-33-treated Cpa3$^{cre/+}$ mice lack mature MCs and markedly reduced numbers of MC progenitors and basophils in the lung compared to IL-33-treated wild-type littermates.

Next, we measured spirometry-like parameters to determine whether MCs contribute to reduced lung function induced by IL-33. There were no differences in FEV 0.1, PEF, FVC, and IC between IL-33-treated Cpa3$^{cre/+}$ and their wild-type littermates (Figure 2e–h). However, methacholine-induced airway resistance was slightly reduced in IL-33-treated Cpa3$^{cre/+}$ mice (Figure 2i). As we previously found a role for MC-derived serotonin (5-HT) in mediating AHR in a model of HDM-induced allergic airway inflammation [12], we accordingly analysed 5-HT levels in BAL. There was a trend ($p = 0.08$) toward a reduction in 5-HT in IL-33-treated Cpa3$^{cre/+}$ mice (Figure 2j). As IL-13 has been shown to be involved in IL-33-induced AHR [24], IL-13 was measured in BAL and lung. However, IL-13 levels were similar in IL-33-treated Cpa3$^{cre/+}$ mice and wild-type littermates (Figure S3a,b). These results suggest that MCs may play a minor role in IL-33-induced AHR.

IL-33-treated MC-deficient Cpa3$^{cre/+}$ mice have reduced BAL T-cells, which is accompanied by reduced CXCL1 and IL-33 levels in the lung

To determine the possible impact of MC deficiency on IL-33-induced airway inflammation, BAL cells were collected from IL-33- or vehicle-treated Cpa3$^{cre/+}$ mice and their wild-type littermates and quantified by flow cytometry. Intranasal IL-33 induced increased CD4^{+} and CD8^{+} T-cells, eosinophils, and neutrophils in both genotypes (Figure 3a–d). Strikingly, IL-33-treated Cpa3$^{cre/+}$ mice displayed a 50% reduction in BAL CD4^{+} and CD8^{+} T-cells compared to the IL-33-treated wild-type littermates (Figure 3a,b). In contrast, there was no difference between the different genotypes in IL-33-induced BAL eosinophils and neutrophils (Figure 3c,d).

To test whether the reduction in BAL T-cells in IL-33-treated Cpa3$^{Cre/+}$ mice was reflected in the lung compartment, T-cells were quantified in the lung. Interestingly, intranasal IL-33 did not alter the total number of CD4^{+} and CD8^{+} lung T-cells from vehicle-treated mice (Figure S3c,d). Notably, the fraction of T-cells that actually transmigrated and ended up in the BAL was minute compared to the total number of lung T-cells. The total lung T-cells also showed a large variation between mice. Together these reasons make a consequent reduction of lung T-cells due to the IL-33-induced transmigration unable to be detected. Nevertheless, our data suggests that in this model, IL-33 stimulated a partly MC-dependent transepithelial migration of lung T-cells to the bronchoalveolar space, but did not induce recruitment of new T-lymphocytes from the vasculature.

To determine which mediator(s) may be causing the MC-enhanced accumulation of BAL T-cells, a cytokine array of lung lysates from IL-33-exposed Cpa3$^{+/+}$ and

13652567, 2024, 3, Downloaded from https://onlinelibrary.wiley.com/doi/10.1111/imm.13849 by Uppsala University Library, Wiley Online Library on [18/02/2025]. See the Terms and Conditions (https://onlinelibrary.wiley.com/terms-and-conditions) on Wiley Online Library for rules of use; OA articles are governed by the applicable Creative Commons License

immunology
Insights into immunity in health and disease

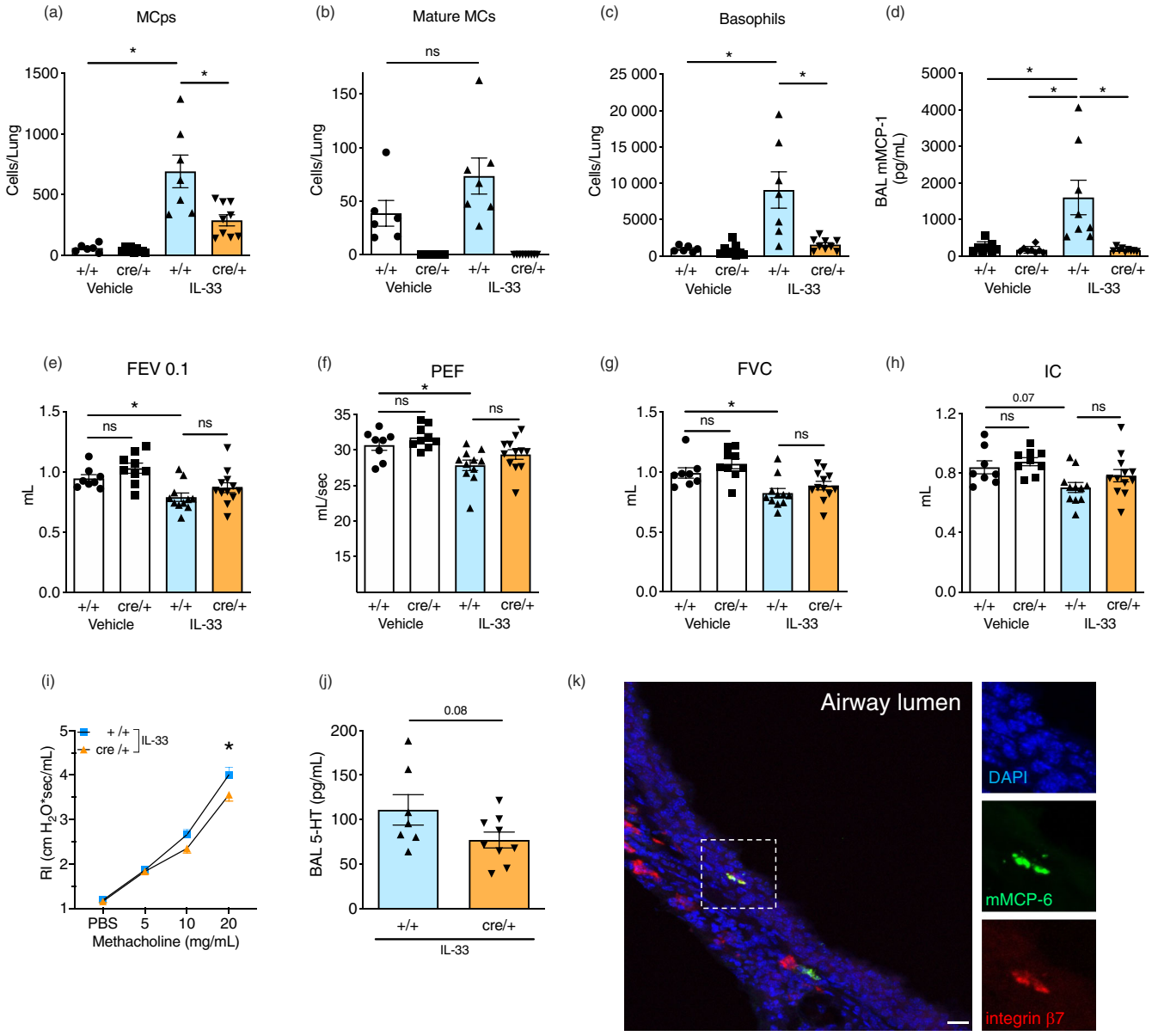

FIGURE 2 Intranasal IL-33 induces accumulation of lung MC progenitors close to the epithelium and AHR, which is reduced in $Cpa3^{cre/+}$ mice. (a–c) The number of lung MC progenitors (MCps) (a), mature MCs (b), and basophils (c) were quantified by flow cytometry in IL-33- or vehicle-treated $Cpa3^{cre/+}$ (cre/+) or $Cpa3^{+/+}$ mice (+/+). (d) The levels of mouse MC protease-1 (mMCP-1) were measured in bronchoalveolar lavage fluid (BAL) from IL-33 exposed mice. (e–h) Spirometry-like parameters forced expired volume in 0.1 s (FEV 0.1) (e), peak of expiratory flow (PEF) (f), forced vital capacity (FVC) (g), and inspiratory capacity (IC) (h) were analysed in $Cpa3^{cre/+}$ and $Cpa3^{+/+}$ mice given IL-33 or vehicle. (i) Airway resistance (RI) to methacholine in $Cpa3^{cre/+}$ ($n = 18$) and $Cpa3^{+/+}$ ($n = 14$) mice exposed to IL-33. (j) 5-HT levels were measured BAL from IL-33-treated $Cpa3^{cre/+}$ and $Cpa3^{+/+}$ mice. (k) A representative picture of a cell immunopositive for mMCP-6 (green) and integrin β7 (red) in the airway epithelium from a representative IL-33-exposed wild-type mouse out of three. The cell nuclei were stained with 4′,6-diamidino-2-phenylindole (DAPI) (blue). Bars represent mean ± SEM of three (a–h, j) or four (i) independent experiments. Scale bar represents 20 μm. Each symbol in (a–h, j) represents data from an individual mouse. Statistical difference was tested by one-way ANOVA with Tukey's post hoc test and only relevant comparisons are shown (a–c, e–h), two-way ANOVA with repeated measurements with Bonferroni's post hoc test (i), or unpaired Student's *t*-test (d, j). $*p < 0.05$; ns, no significant difference.

$Cpa3^{cre/+}$ mice was performed. The most prominent difference was a ~2-fold reduction in CXCL1 in the lungs of IL-33-treated $Cpa3^{cre/+}$ mice (Figure S3e), which was confirmed by ELISA (Figure 3e). Nevertheless, the levels of CXCL1 in the BAL were similar in IL-33-exposed $Cpa3^{cre/+}$ and $Cpa3^{+/+}$ mice, but approximately 5–10 times higher in BAL than in the lung (Figure 3f).

Next, lung IL-33 levels were quantified by ELISA. The IL-33 levels were reduced in the lung from IL-33-treated $Cpa3^{cre/+}$ mice as compared to their wild-type littermates

13652567, 2024, 3, Downloaded from https://onlinelibrary.wiley.com/doi/10.1111/imm.13849 by Uppsala University Library, Wiley Online Library on [18/02/2025]. See the Terms and Conditions (https://onlinelibrary.wiley.com/terms-and-conditions) on Wiley Online Library for rules of use; OA articles are governed by the applicable Creative Commons License

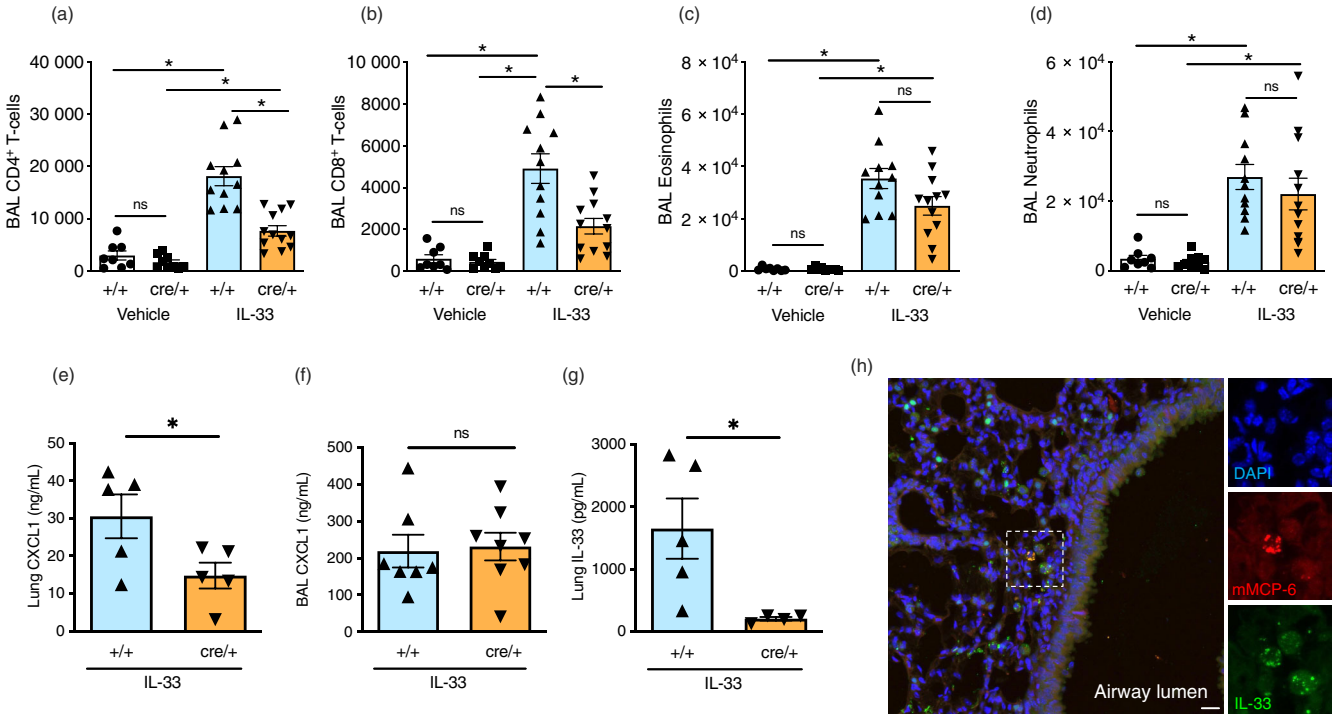

FIGURE 3 IL-33-treated Cpa3$^{cre/+}$ mice have reduced CD4$^+$ and CD8$^+$ BAL T-cells accompanied by reduced IL-33 and CXCL1 levels in the lung. (a–d) The number of CD4$^+$ (A) and CD8$^+$ T-cells (b), eosinophils (c), and neutrophils (d) in BAL was quantified by flow cytometry in IL-33- or vehicle-treated Cpa3$^{cre/+}$ (cre/+) and Cpa3$^{+/+}$ mice (+/+). (e–g) CXCL1 in lung (e) and BAL (f), and lung IL-33 (g) levels were quantified by ELISA in mice that received IL-33. (H) A representative picture of a cell immunopositive for mMCP-6 (red) and IL-33 (green) close to the airway epithelium of an IL-33-exposed wild-type mouse out of three analysed. The cell nuclei were stained with 4′,6-diamidino-2-phenylindole (DAPI) (blue). Bars represent mean ± SEM of two (e, g) and three (a–d, f) pooled independent experiments. Each symbol represents data from an individual mouse. Statistical difference was tested by one-way ANOVA with Tukey post hoc test and only relevant comparisons are shown (a–d) or unpaired Student's *t*-test (e–g). *$p < 0.05$; ns, no significant difference.

treated in parallel (Figure 3g). Moreover, IL-33$^+$ mMCP-6$^+$ MCs were found near the airway epithelium in wild-type mice treated with IL-33 (Figure 3h). This suggests an amplifying role for IL-33-producing MCs in the IL-33-induced lung pathology. To summarize, intranasal IL-33 establishes a CXCL1 gradient from the lung to the bronchoalveolar space and induces IL-33$^+$ MCs localized to the epithelium. Further, IL-33-treated Cpa3$^{cre/+}$mice have a reduction in BAL T-cells, which is accompanied by less IL-33 and CXCL1 in the lungs.

IL-33 induces CXCR2 expression in lung and BAL T-cells independent of MCs

To determine whether the CXCL1/CXCR2 axis could be involved in the IL-33-induced mobilization of T-cells from the lung to bronchoalveolar space, we investigated whether these T-cells expressed CXCR2. Indeed, lung T-cells from IL-33-treated mice showed induced CXCR2 surface expression (Figure 4a). However, the IL-33-induced stimulation of CXCR2 expression in T-cells was independent of MCs as intranasal IL-33 induced a 4-fold increase in the percentage of CXCR2$^+$ CD4$^+$ and CD8$^+$ lung T-cells in both genotypes (Figure 4b,c). Due to extremely low BAL T-cell numbers in the vehicle control mice, such a comparison was not possible in BAL. Nevertheless, CXCR2 expression was prominent in BAL CD4$^+$ and CD8$^+$ cells from IL-33-treated mice with around 7%–8% cells showing CXCR2 surface expression. Thus, CXCR2-expressing T-cells are ∼5-fold more common in BAL than in the lung, which could mean that T-cells translocating to the bronchoalveolar space use the CXCL1/CXCR2 axis for their directed migration. To determine whether CXCR2-expressing T-cells are also a feature of allergic airway inflammation, mice were given four intranasal administrations of HDM over 10 days, and the lung and BAL T-cells were analysed 1 day after the final HDM administration. Again, a higher proportion of around 4%–7% CXCR2-positive CD4$^+$ and CD8$^+$ T-cells were found in BAL compared to lung tissue (Figure S4a,b). For comparison, around 2%–5% of BAL neutrophils were also immune positive for surface-associated CXCR2 (Figure S4c).

13652567, 2024, 3, Downloaded from https://onlinelibrary.wiley.com/doi/10.1111/imm.13849 by Uppsala University Library, Wiley Online Library on [18/02/2025]. See the Terms and Conditions (https://onlinelibrary.wiley.com/terms-and-conditions) on Wiley Online Library for rules of use; OA articles are governed by the applicable Creative Commons License

immunology
Insights into immunity in health and disease

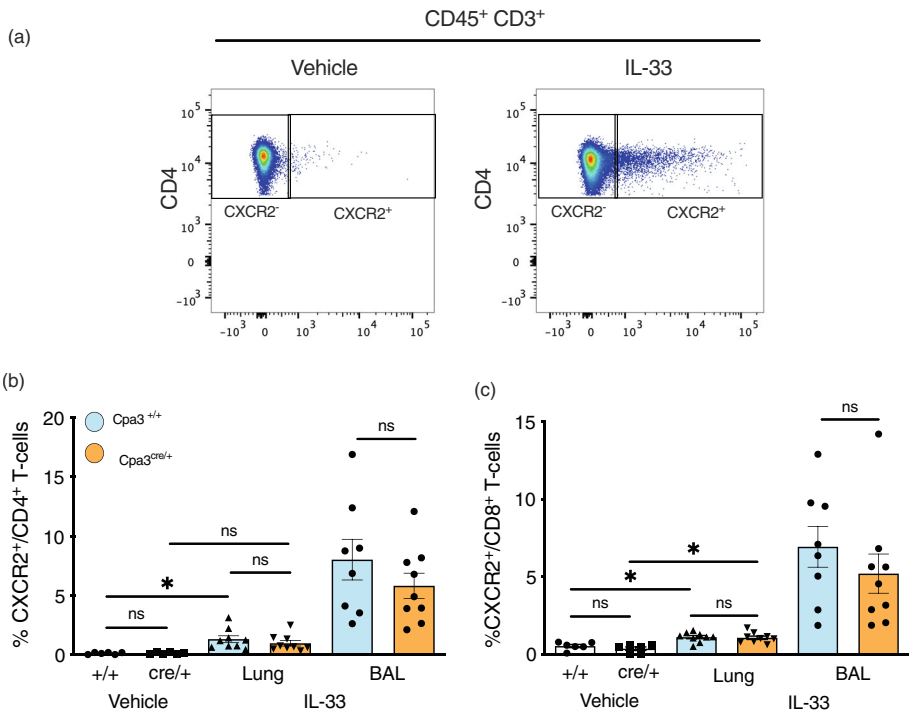

FIGURE 4 Intranasal IL-33 induces surface-associated CXCR2 in T-cells. (a–c) The proportion of CXCR2$^+$ cells among CD4$^+$ (a, b) or CD8$^+$ (CD3$^+$ CD45$^+$) T-cells (c) was quantified by flow cytometry in the lung and bronchoalveolar lavage fluid (BAL). (a) shows the gating of CXCR2$^+$ and CXCR2$^-$ CD4$^+$ T-cells in lung cells from a representative vehicle control and an IL-33-treated Cpa3$^{+/+}$ mouse. (b, c) For vehicle-treated mice, T-cells were only detectable in the lung samples. Bars represent mean ± SEM of three pooled independent experiments. Each symbol represents data from an individual mouse. Statistical differences were tested by one-way ANOVA with Tukey post hoc test (b, c) and only relevant comparisons are shown. *$p < 0.05$; ns, no significant difference.

Subsequently, we tested whether IL-33-induced CXCR2-surface expression in T-cells is associated with a certain T-cell subset. When T-cells from IL-33-treated mice were divided based on their CXCR2 surface expression, around 10% of CXCR2$^+$ and CXCR2$^-$ CD4$^+$ T-cells were ST2$^+$ (Figure 5a; Figure S4d), whereas 30% and 15% of the CXCR2$^+$ and CXCR2$^-$ CD8$^+$ T-cells, respectively, were ST2$^+$ (Figure 5b). However, since there are fewer CD8$^+$ than CD4$^+$ T-cells in the lung, approximately the same total number of CXCR2$^+$ ST2$^+$ CD4$^+$ and CD8$^+$ T-cells were found in the mice subjected to IL-33.

ST2-mediated IL-33 signalling has been reported for FoxP3$^+$ T-regs and GATA-3$^+$ Th2 cells [25, 26]. To determine whether CXCR2 expression was associated with T-regs, Th2 cells, or both, the proportion of FoxP3$^+$ and GATA-3$^+$ populations in CXCR2$^+$ and CXCR2$^-$ CD4$^+$ lung T-cells were analysed. Similar fractions of CXCR2$^+$ and CXCR2$^-$ CD4$^+$ T-cells were FoxP3$^+$ (1.3% ± 1.0% vs. 1.8% ± 0.9%) (Figure 5c,d), and GATA-3$^+$ (0.6% ± 0.5% vs. 0.5% ± 0.2%) in the lungs from IL-33-treated wild-type mice (Figure S4d–f). In summary, IL-33 induces CXCR2-expressing T-cells, which are enriched in BAL. Further, induction of CXCR2 seems to be a general phenomenon for several kinds of T-cells in mouse lungs with type 2 inflammation.

Lung MCs colocalize with CXCL1 in vivo

To determine whether lung MCs in IL-33-treated mice provide CXCL1 and to establish where they are located, lung sections from IL-33-treated wild-type mice were analysed by immunofluorescence microscopy. MCs positive for mMCP-6 that also stained positive for CXCL1 localized primarily in or close to the lung epithelium (Figure 5e, left panel) and in the submucosal area close to the epithelium (Figure 5e, middle panel). CXCL1 was also expressed in mMCP-8$^+$ cells in the lung parenchyma (Figure 5e, right panel). The protease mMCP-8 is expressed by basophils and MC progenitors in the lung [27]. These results suggest that MCs display CXCL1 in close proximity to the epithelium, and that MCs, their progenitors and potentially basophils are sources of this chemokine in mice with IL-33-induced airway inflammation.

DISCUSSION

IL-33 has emerged as an important target in respiratory diseases. So far, the IL-33 neutralizing antibody, itepekimab, has been shown to improve asthma control, quality of life, and lung function in patients with moderate to severe asthma [28], as well as to reduce chronic obstructive pulmonary disease (COPD) exacerbations in former smokers [29]. Given the promising data on targeting IL-33 in asthma and COPD patients, it is important to elucidate the underlying mechanisms. We hypothesized that IL-33-stimulated MCs mediate pathological effects in respiratory diseases. In the current study, we investigated this hypothesis experimentally using intranasal delivery of IL-33 to mice. Our findings suggest that MCs

13652567, 2024, 3, Downloaded from https://onlinelibrary.wiley.com/doi/10.1111/imm.13849 by Uppsala University Library, Wiley Online Library on [18/02/2025]. See the Terms and Conditions (https://onlinelibrary.wiley.com/terms-and-conditions) on Wiley Online Library for rules of use; OA articles are governed by the applicable Creative Commons License

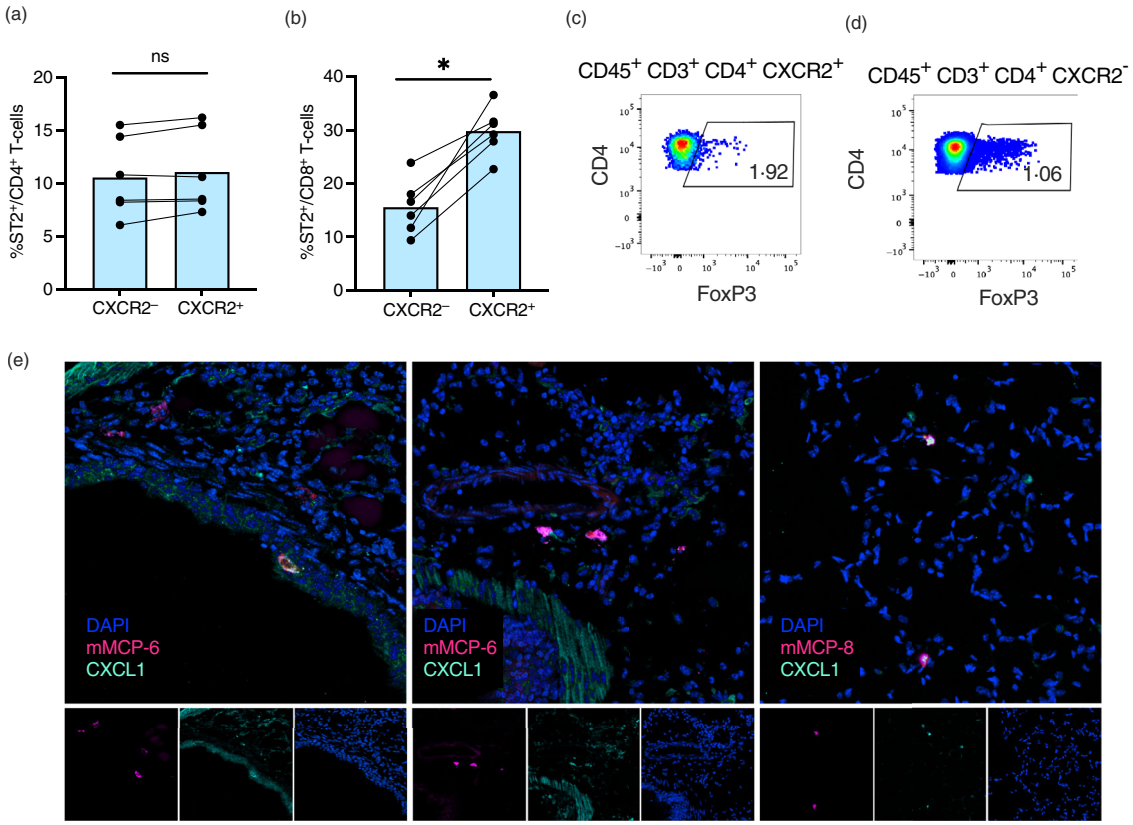

FIGURE 5 Lung MCs co-localize with CXCL1 in IL-33-exposed mice. (a, b) The proportion of $ST2^+$ cells among $CXCR2^+$ and $CXCR2^-$ $CD4^+$ (a) or $CD8^+$ (b) lung T-cells from IL-33 treated BALB/c mice. (c, d) Representative gating of intracellular FoxP3 in $CXCR2^+$ (c) and $CXCR2^-$ (d) $CD4^+$ lung T-cells from a representative IL-33 treated BALB/c mouse ($n = 6$) from three experiments. (e) Representative lung sections from IL-33-treated BALB/c mice ($n = 3$) stained with antibodies recognizing mouse CXCL1 (cyan), mMCP-6 (MC magenta), or mMCP-8 (basophil marker, magenta). The cell nuclei were stained with 4′,6-diamidino-2-phenylindole (DAPI) (blue). Minimized single channel images are shown in the bottom panels (e). Scale bar represents 20 μm. (a, b) Each symbol represents data from an individual mouse. Statistical difference was tested by paired Student's *t*-test. $^*p < 0.05$.

contribute to IL-33-induced airway inflammation, thereby providing further insights into the mechanisms behind the therapeutic benefit of IL-33 modulation in respiratory conditions.

Given the appropriate location of MCs in or close to the epithelial barrier in respiratory diseases, MCs have been previously suggested to play a detrimental role in IL-33-induced lung pathology. For example, gene expression of type 2 cytokines IL-4, IL-5, and IL-13 correlates with MC gene expression (TPSAB1, CPA3) in induced sputum cells and bronchial brushings from patients with asthma, and IL-33 induced production of type 2 cytokines occurs in human cord blood-derived MCs [30]. Further, ST2 gene expression in epithelial brushings correlated positively with the density of epithelial MCs in asthma patients with exercise-induced AHR [31]. Nevertheless, an ST2-independent action of oxidized IL-33, which mediates epithelial remodelling and mucin hypersecretion, has been recently reported, illustrating the complex actions of IL-33 [32]. Still, the potential involvement of $ST2^+$ MCs in IL-33-induced airway inflammation and associated impairment of lung function induced by IL-33 had remained unclear.

Our current study demonstrates for the first time that intranasal IL-33 administrations alone induce a ST2-dependent reduction in the spirometry-like lung function parameters. Since these lung function parameters were intact in IL-33-treated $Cpa3^{cre/+}$ mice, ST2-expressing cells other than MCs primarily drive the processes responsible for the IL-33-induced decline in spirometry-like lung function. AHR is another critical hallmark of asthma, and a feature sometimes also present in COPD. A link between IL-33-activated MCs and AHR was suggested in a study where concomitant administration of IL-33 and ovalbumin exacerbated AHR, an effect that was lost in MC-deficient $Kit^{W-sh/W-sh}$ mice [33]. Intranasal IL-33 alone also induced AHR in mice in absence of adaptive immunity [17], and this was at least partly mediated by IL-13 [24]. Kaur et al also showed that IL-33-induced AHR was associated with increased levels of mMCP-1 in serum, suggesting MC activation. In agreement, we found increased mMCP-1 levels in BAL from

13652567, 2024, 3, Downloaded from https://onlinelibrary.wiley.com/doi/10.1111/imm.13849 by Uppsala University Library, Wiley Online Library on [18/02/2025]. See the Terms and Conditions (https://onlinelibrary.wiley.com/terms-and-conditions) on Wiley Online Library for rules of use; OA articles are governed by the applicable Creative Commons License

IL-33-treated wild-type mice, but this mucosal MC protease was barely detectable in IL-33-treated Cpa3$^{cre/+}$ mice. However, IL-33-treated Cpa3$^{cre/+}$ mice only showed a small reduction in AHR to methacholine, along with intact IL-13 levels. This contrasts with our previous study where 50% reduction in AHR was found in Cpa3$^{cre/+}$ mice with acute HDM-induced allergic airway inflammation [12]. Key factors that may explain the vital contribution of MCs to AHR in allergen-induced inflammation compared to IL-33-induced inflammation include the 5-10-fold higher abundance of lung MCs, and the stronger mode of IgE-mediated MC activation in the HDM-induced lung inflammation model. In the HDM model, the MC contribution to AHR was related to MC-derived 5-HT. However, only a tendency of decreased 5-HT levels was found in BAL fluid from IL-33-treated Cpa3$^{cre/+}$ mice. Therefore, MC-derived 5-HT seems to play a non-significant role in AHR in mice induced by IL-33 alone. Nevertheless, as the intranasal IL-33 model led to 8-fold higher levels of lung-associated IL-33 in MC-sufficient Cpa3$^{+/+}$ compared to Cpa3$^{cre/+}$ mice, a possibility is that MCs contribute to AHR by amplifying IL-33. A role for MC-derived IL-33 was previously found in amplifying the ILC2-mediated clearance of helminths in the gut [34]. Further, mMCP-1 from intraepithelial MCs was recently shown to be taken up in gut-lining epithelial cells, cleaving and activating gasdermin C, which was needed for the secretion of IL-33 during helminth infection [35]. Thus, MC-derived or facilitated IL-33 release may fuel other innate ST2$^+$ immune cells, such as ILC2s, which are directly responsible for the MC-enhanced IL-33-induced AHR [36].

Airway inflammation is a feature of IL-33-associated respiratory diseases, which involves recruitment of immune cells through transendothelial migration into the lung, followed by transepithelial migration to the bronchoalveolar space. The egression of T-cells into the alveolar space occurs as a response to inflammatory triggers that creates chemokine gradients, allowing T-cells to traverse both disrupted and intact bronchial epithelium [37, 38]. Importantly, our data suggest that CD4$^+$ and CD8$^+$ T-cells primarily transmigrate from the lung to the bronchoalveolar space in response to intranasal IL-33. However, in MC-deficient mice subjected to IL-33, transmigration of T-cells to the bronchoalveolar space was reduced by around 50%. Moreover, we observed a reduction in CXCL1 levels in the lungs of the IL-33-treated Cpa3$^{cre/+}$ mice, suggesting a link between T-cell migration, CXCL1, and MCs.

From previous studies, several CXCR2-binding chemokines are widely known as a neutrophil chemoattractants [39–41]. However, in our model, only CXCL1 was detectable. MCs have been shown to mediate neutrophil recruitment by releasing CXCL1 in other inflammatory settings [42–45], and more recently to drive the reverse transendothelial migration of neutrophils in aged inflamed tissues [46]. While we also detected CXCR2 surface expression in neutrophils by flow cytometry, the influx of neutrophils to BAL was not affected by MC deficiency 4 days after the first IL-33 administration, which was when we detected the reduction of BAL T-cells. Our assessment at 4 days post IL-33 administration contrasts with earlier studies where an effect on neutrophil accumulation mediated by resident connective tissue type MCs was triggered by other means at much earlier time points [43–46]. Instead, our study specifically focuses on the contribution of inflammation-induced MC progenitors and mucosal MCs in the context of IL-33-induced inflammation in the airways. These distinctions in experimental parameters and tissue specificity underscore the nuanced and context-dependent nature of MC involvement in immune responses.

In the present study, intranasal IL-33 induced CXCR2 surface expression in both CD4$^+$ and CD8$^+$ T and were a consistent feature among different T-cell subtypes. The CXCR2/CXCL1 axis has been previously implicated in CD4$^+$ T-cell mobilization during neuroinflammatory conditions in a mouse model of multiple sclerosis [47]. Furthermore, CXCL1 mediated mobilization of CXCR2$^+$ human T-regs in vitro in a chemotaxis assay [48]. In our study, a higher level of CXCL1 and a larger fraction of CXCR2$^+$ T-cells were found in the bronchoalveolar compartment than in the lung of IL-33-exposed wild-type mice, implying CXCR2$^+$ T-cells following a CXCL1 gradient. Similarly, Thomas et al described that the proportion of CXCR2-expressing CD4$^+$ and CD8$^+$ T-cells is higher in BAL than in peripheral blood from patients with allergic asthma [49]. Importantly, we found mMCP-6$^+$ CXCL1$^+$ MCs localized near the airway epithelium of IL-33-treated wild-type mice and a marked reduction of BAL T-cells and lung CXCL1 in IL-33-treated MC deficient mice. Thus, we speculate that the loss of MCs displaying CXCL1 close to the epithelium disrupts the delicate balance of bioavailable CXCL1 at this site, which is necessary for intact lung T-cell chemotaxis to the epithelium. Therefore, we postulate that the lack of CXCL1$^+$ MCs prevents an intact T-cell transmigration to the bronchoalveolar space. However, the precise mechanism of T-cell migration in this model remains a subject of ongoing investigation.

A limitation of our study is that the IL-33-treated Cpa3$^{cre/+}$ mice do not only lack MCs and show a strong reduction in lung MC progenitors but also show a reduction in lung basophils. A decrease in splenic basophils was previously noted already in the original paper describing the Cpa3$^{cre/+}$ strain [21]. In the IL-33

13652567, 2024, 3, Downloaded from https://onlinelibrary.wiley.com/doi/10.1111/imm.13849 by Uppsala University Library, Wiley Online Library on [18/02/2025]. See the Terms and Conditions (https://onlinelibrary.wiley.com/terms-and-conditions) on Wiley Online Library for rules of use; OA articles are governed by the applicable Creative Commons License

model, it is also possible that MCs are involved in the inflammation-induced influx of basophils to the lung. Still, since basophils also express ST2, they might also contribute with CXCL1 in IL-33-induced airway inflammation. The mouse protease mMCP-8 has been widely used as a basophil marker and as a target in transgenic mice to deplete basophils in vivo [50]. In fact, we detected mMCP-8$^+$ CXCL1$^+$ cells confined to the lung parenchyma in wild-type mice subjected to intranasal IL-33. However, some MC progenitors in the lung also express mMCP-8, and we previously showed that depletion of Mcpt8-expressing cells resulted in reduced lung MC progenitors, an effect that was translated to a decrease in MCs at a later time point, in HDM-induced allergic airway inflammation [27]. Therefore, the CXCL1-expressing mMCP-8$^+$ cells in the IL-33-exposed lungs might consist of basophils, MC progenitors, or both. Nevertheless, the CXCL1$^+$ mMCP-6$^+$ MCs in lung sections from IL-33-exposed mice were mainly localized in the submucosa, close to the epithelial barrier, or in the epithelium. In these places, we could not detect any mMCP-8$^+$ cells. Another limitation of our study is that we did not directly demonstrate that lung MCs in vivo produce CXCL1 in IL-33-induced airway inflammation. Mucosal MCs express highly sulfated chondroitin sulfate proteoglycans [51]. Hence, it is possible that the CXCL1 is produced by another cell type, associates to and become displayed by lung MCs close to the epithelium.

In summary, intranasal IL-33 induces MC accumulation and activation, increases CXCL1 levels, and augments CXCR2 surface expression in lung T-cells. The reduced CXCL1 levels in MC deficient mice together with the presence of CXCL1$^+$ MCs close to or in the epithelium of IL-33-exposed wild-type mice compasses findings that are compatible with a mechanism in which MC-derived or displayed CXCL1 mediates the localization of CXCR2-bearing T-cells close to the epithelium. Hence, MCs may be assisting T-cells in sensing and responding to even more elevated levels of CXCL1 in the bronchoalveolar space, thereby leading to their epithelial transmigration. Thus, our study suggests that MCs at the respiratory epithelial surfaces mediate IL-33-induced pathological effects that may be significant in IL-33-related airway diseases.

AUTHOR CONTRIBUTIONS

JH, EM-E, and PAA-V conceived and designed the study. PAA-V performed all experiments presented in the main figures, designed, and analysed experiments. The initial experiments were performed by EM-E and LP as part of LPs bachelor project. DP-C and AD participated in one set of experiments each. PAA-V and JH wrote the manuscript. All authors critically assessed and approved the manuscript.

ACKNOWLEDGEMENTS

The authors wish to thank Thomas Plum for fruitful discussions and Andrew McKenzie, Thorsten Feyerabend, and Hans-Reimer Rodewald for providing the ST2$^{-/-}$ and Cpa3$^{cre/+}$ mice, respectively. Flow cytometry was performed on equipment provided by the BioVis Facility, Uppsala, Sweden.

FUNDING INFORMATION

This work was supported by grants to JH from the Swedish Research Council (2016-00803; 2023-01848), the Swedish Cancer Society (22 21 15), Knut and Alice Wallenberg Foundation (2017.0022), Ruth and Nils-Erik Stenbäck Foundation, Konsul ThC Bergh's Foundation, and Hans von Kantzow Foundation.

CONFLICT OF INTEREST STATEMENT

The authors declare no conflict of interests.

DATA AVAILABILITY STATEMENT

The data that support the findings of this study are available from the corresponding author upon reasonable request.

ORCID

P. Abigail Alvarado-Vazquez https://orcid.org/0000-0003-4623-3478
Erika Mendez-Enriquez https://orcid.org/0000-0002-2114-2812
Aleksandra Dondalska https://orcid.org/0000-0003-3259-634X
Diego Pazos-Castro https://orcid.org/0000-0002-0686-5131
Jenny Hallgren https://orcid.org/0000-0002-3685-5364

REFERENCES

1. Cayrol C, Girard JP. Interleukin-33 (IL-33): a critical review of its biology and the mechanisms involved in its release as a potent extracellular cytokine. Cytokine. 2022;156:155891.
2. Guo L, Wei G, Zhu J, Liao W, Leonard WJ, Zhao K, et al. IL-1 family members and STAT activators induce cytokine production by Th2, Th17, and Th1 cells. Proc Natl Acad Sci U S A. 2009;106:13463–8.
3. Arpaia N, Green JA, Moltedo B, Arvey A, Hemmers S, Yuan S, et al. A distinct function of regulatory T cells in tissue protection. Cell. 2015;162:1078–89.
4. Moffatt MF, Gut IG, Demenais F, Strachan DP, Bouzigon E, Heath S, et al. A large-scale, consortium-based genomewide association study of asthma. N Engl J Med. 2010;363:1211–21.
5. Li Y, Wang W, Lv Z, Li Y, Chen Y, Huang K, et al. Elevated expression of IL-33 and TSLP in the Airways of Human

13652567, 2024, 3, Downloaded from https://onlinelibrary.wiley.com/doi/10.1111/imm.13849 by Uppsala University Library, Wiley Online Library on [18/02/2025]. See the Terms and Conditions (https://onlinelibrary.wiley.com/terms-and-conditions) on Wiley Online Library for rules of use; OA articles are governed by the applicable Creative Commons License

Asthmatics in Vivo: a potential biomarker of severe refractory disease. J Immunol. 2018;200:2253–62.
6. Momen T, Ahanchian H, Reisi M, Shamsdin SA, Shahsanai A, Keivanfar M. Comparison of Interleukin-33 serum levels in asthmatic patients with a control group and relation with the severity of the disease. Int J Prev Med. 2017;8:65.
7. Dougherty RH, Sidhu SS, Raman K, Solon M, Solberg OD, Caughey GH, et al. Accumulation of intraepithelial mast cells with a unique protease phenotype in T(H)2-high asthma. J Allergy Clin Immunol. 2010;125:1046–1053 e8.
8. Brightling CE, Bradding P, Symon FA, Holgate ST, Wardlaw AJ, Pavord ID. Mast-cell infiltration of airway smooth muscle in asthma. N Engl J Med. 2002;346:1699–705.
9. Abonia JP, Hallgren J, Jones T, Shi T, Xu Y, Koni P, et al. Alpha-4 integrins and VCAM-1, but not MAdCAM-1, are essential for recruitment of mast cell progenitors to the inflamed lung. Blood. 2006;108:1588–94.
10. Hallgren J, Jones TG, Abonia JP, Xing W, Humbles A, Austen KF, et al. Pulmonary CXCR2 regulates VCAM-1 and antigen-induced recruitment of mast cell progenitors. Proc Natl Acad Sci U S A. 2007;104:20478–83.
11. Dahlin JS, Feinstein R, Cui Y, Heyman B, Hallgren J. CD11c+ cells are required for antigen-induced increase of mast cells in the lung. J Immunol. 2012;189:3869–77.
12. Mendez-Enriquez E, Alvarado-Vazquez PA, Abma W, Simonson OE, Rodin S, Feyerabend TB, et al. Mast cell-derived serotonin enhances methacholine-induced airway hyperresponsiveness in house dust mite-induced experimental asthma. Allergy. 2021;76:2057–69.
13. Iikura M, Suto H, Kajiwara N, Oboki K, Ohno T, Okayama Y, et al. IL-33 can promote survival, adhesion and cytokine production in human mast cells. Lab Invest. 2007;87:971–8.
14. Ho LH, Ohno T, Oboki K, Kajiwara N, Suto H, Iikura M, et al. IL-33 induces IL-13 production by mouse mast cells independently of IgE-FcepsilonRI signals. J Leukoc Biol. 2007;82:1481–90.
15. Andrade MV, Iwaki S, Ropert C, Gazzinelli RT, Cunha-Melo JR, Beaven MA. Amplification of cytokine production through synergistic activation of NFAT and AP-1 following stimulation of mast cells with antigen and IL-33. Eur J Immunol. 2011;41:760–72.
16. Hsu C-L, Neilsen CV, Bryce PJ. IL-33 is produced by mast cells and regulates IgE-dependent inflammation. PLoS ONE. 2010;5:e11944.
17. Kondo Y, Yoshimoto T, Yasuda K, Futatsugi-Yumikura S, Morimoto M, Hayashi N, et al. Administration of IL-33 induces airway hyperresponsiveness and goblet cell hyperplasia in the lungs in the absence of adaptive immune system. Int Immunol. 2008;20:791–800.
18. Salmond RJ, Mirchandani AS, Besnard AG, Bain CC, Thomson NC, Liew FY. IL-33 induces innate lymphoid cell-mediated airway inflammation by activating mammalian target of rapamycin. J Allergy Clin Immunol. 2012;130:1159–1166 e6.
19. Zarnegar B, Westin A, Evangelidou S, Hallgren J. Innate immunity induces the accumulation of lung mast cells during influenza infection. Front Immunol. 2018;9:2288.
20. Méndez-Enríquez E, Salomonsson M, Eriksson J, Janson C, Malinovschi A, Sellin ME, et al. IgE cross-linking induces activation of human and mouse mast cell progenitors. J Allergy Clin Immunol. 2022;149:1458–63.
21. Feyerabend TB, Weiser A, Tietz A, Stassen M, Harris N, Kopf M, et al. Cre-mediated cell ablation contests mast cell contribution in models of antibody- and T cell-mediated autoimmunity. Immunity. 2011;35:832–44.
22. Townsend MJ, Fallon PG, Matthews DJ, Jolin HE, McKenzie AN. T1/ST2-deficient mice demonstrate the importance of T1/ST2 in developing primary T helper cell type 2 responses. J Exp Med. 2000;191:1069–76.
23. Alvarado-Vazquez PA, Mendez-Enriquez E, Hallgren J. Use of spirometry-like measurements to monitor house dust mite-induced experimental asthma in mice. Allergy. 2021;76:2204–7.
24. Kaur D, Gomez E, Doe C, Berair R, Woodman L, Saunders R, et al. IL-33 drives airway hyper-responsiveness through IL-13-mediated mast cell: airway smooth muscle crosstalk. Allergy. 2015;70:556–67.
25. Schiering C, Krausgruber T, Chomka A, Fröhlich A, Adelmann K, Wohlfert EA, et al. The alarmin IL-33 promotes regulatory T-cell function in the intestine. Nature. 2014;513:564–8.
26. Hayakawa M, Yanagisawa K, Aoki S, Hayakawa H, Takezako N, Tominaga S. T-helper type 2 cell-specific expression of the ST2 gene is regulated by transcription factor GATA-3. Biochim Biophys Acta. 2005;1728:53–64.
27. Alvarado-Vazquez PA, Cardenas EI, Das A, Hallgren J. Depletion of Mcpt8-expressing cells reduces lung mast cells in mice with experimental asthma. Allergy. 2023;78:1363–6.
28. Wechsler ME, Ruddy MK, Pavord ID, Israel E, Rabe KF, Ford LB, et al. Efficacy and safety of Itepekimab in patients with moderate-to-severe asthma. N Engl J Med. 2021;385:1656–68.
29. Rabe KF, Celli BR, Wechsler ME, Abdulai RM, Luo X, Boomsma MM, et al. Safety and efficacy of itepekimab in patients with moderate-to-severe COPD: a genetic association study and randomised, double-blind, phase 2a trial. Lancet Respir Med. 2021;9:1288–98.
30. Altman MC, Lai Y, Nolin JD, Long S, Chen CC, Piliponsky AM, et al. Airway epithelium-shifted mast cell infiltration regulates asthmatic inflammation via IL-33 signaling. J Clin Invest. 2019;129:4979–91.
31. Murphy RC, Lai Y, Liu M, Al-Shaikhly T, Altman MC, Altemeier WA, et al. Distinct epithelial-innate immune cell transcriptional circuits underlie airway Hyperresponsiveness in asthma. Am J Respir Crit Care Med. 2023;207:1565–75.
32. Strickson S, Houslay KF, Negri VA, Ohne Y, Ottosson T, Dodd RB, et al. Oxidised IL-33 drives COPD epithelial pathogenesis via ST2-independent RAGE/EGFR signalling complex. Eur Respir J. 2023;62:2202210.
33. Sjoberg LC, Gregory JA, Dahlen SE, Nilsson GP, Adner M. Interleukin-33 exacerbates allergic bronchoconstriction in the mice via activation of mast cells. Allergy. 2015;70:514–21.
34. Shimokawa C, Kanaya T, Hachisuka M, Ishiwata K, Hisaeda H, Kurashima Y, et al. Mast cells are crucial for induction of group 2 innate lymphoid cells and clearance of helminth infections. Immunity. 2017;46:863–874 e4.
35. Yang L, He H, Guo XK, Wang J, Wang W, Li D, et al. Intraepithelial mast cells drive gasdermin C-mediated type 2 immunity. Immunity. 2024;57:1056–1070 e5.

13652567, 2024, 3, Downloaded from https://onlinelibrary.wiley.com/doi/10.1111/imm.13849 by Uppsala University Library, Wiley Online Library on [18/02/2025]. See the Terms and Conditions (https://onlinelibrary.wiley.com/terms-and-conditions) on Wiley Online Library for rules of use; OA articles are governed by the applicable Creative Commons License

36. Kim HY, Chang YJ, Subramanian S, Lee HH, Albacker LA, Matangkasombut P, et al. Innate lymphoid cells responding to IL-33 mediate airway hyperreactivity independently of adaptive immunity. J Allergy Clin Immunol. 2012;129:216–27.
37. Porter JC, Falzon M, Hall A. Polarized localization of epithelial CXCL11 in chronic obstructive pulmonary disease and mechanisms of T cell egression. J Immunol. 2008;180:1866–77.
38. Persson CG, Uller L. Resolution of cell-mediated airways diseases. Respir Res. 2010;11:75.
39. Sawant KV, Xu R, Cox R, Hawkins H, Sbrana E, Kolli D, et al. Chemokine CXCL1-mediated neutrophil trafficking in the lung: role of CXCR2 activation. J Innate Immun. 2015;7:647–58.
40. Sawant KV, Sepuru KM, Lowry E, Penaranda B, Frevert CW, Garofalo RP, et al. Neutrophil recruitment by chemokines Cxcl1/KC and Cxcl2/MIP2: role of Cxcr2 activation and glycosaminoglycan interactions. J Leukoc Biol. 2021;109:777–91.
41. Nouailles G, Dorhoi A, Koch M, Zerrahn J, Weiner J 3rd, Faé KC, et al. CXCL5-secreting pulmonary epithelial cells drive destructive neutrophilic inflammation in tuberculosis. J Clin Invest. 2014;124:1268–82.
42. Biedermann T, Kneilling M, Mailhammer R, Maier K, Sander CA, Kollias G, et al. Mast cells control neutrophil recruitment during T cell-mediated delayed-type hypersensitivity reactions through tumor necrosis factor and macrophage inflammatory protein 2. J Exp Med. 2000;192:1441–52.
43. De Filippo K, Dudeck A, Hasenberg M, Nye E, van Rooijen N, Hartmann K, et al. Mast cell and macrophage chemokines CXCL1/CXCL2 control the early stage of neutrophil recruitment during tissue inflammation. Blood. 2013;121:4930–7.
44. Nouailles G, Dorhoi A, Koch M, Zerrahn J, Weiner J 3rd, Faé KC, et al. Mast cells mediate neutrophil recruitment during atherosclerotic plaque progression. Atherosclerosis. 2015;241:289–96.
45. Ngo Nyekel F, Pacreau E, Benadda S, Msallam R, Abrink M, Pejler G, et al. Mast cell degranulation exacerbates skin rejection by enhancing neutrophil recruitment. Front Immunol. 2018;9:2690.
46. Barkaway A, Rolas L, Joulia R, Bodkin J, Lenn T, Owen-Woods C, et al. Age-related changes in the local milieu of inflamed tissues cause aberrant neutrophil trafficking and subsequent remote organ damage. Immunity. 2021;54:1494–1510 e7.
47. Khaw YM, Tierney A, Cunningham C, Soto-Díaz K, Kang E, Steelman AJ, et al. Astrocytes lure CXCR2-expressing CD4. Proc Natl Acad Sci U S A. 2021;118:e2017213118.
48. Lv M, Xu Y, Tang R, Ren J, Shen S, Chen Y, et al. miR141-CXCL1-CXCR2 signaling-induced Treg recruitment regulates metastases and survival of non-small cell lung cancer. Mol Cancer Ther. 2014;13:3152–62.
49. Thomas SY, Banerji A, Medoff BD, Lilly CM, Luster AD. Multiple chemokine receptors, including CCR6 and CXCR3, regulate antigen-induced T cell homing to the human asthmatic airway. J Immunol. 2007;179:1901–12.
50. Nouailles G, Dorhoi A, Koch M, Zerrahn J, Weiner J 3rd, Faé KC, et al. Genetic analysis of basophil function in vivo. Nat Immunol. 2011;12:527–35.
51. Braga T, Grujic M, Lukinius A, Hellman L, Abrink M, Pejler G. Serglycin proteoglycan is required for secretory granule integrity in mucosal mast cells. Biochem J. 2007;403:49–57.

SUPPORTING INFORMATION

Additional supporting information can be found online in the Supporting Information section at the end of this article.

How to cite this article: Alvarado-Vazquez PA, Mendez-Enriquez E, Pähn L, Dondalska A, Pazos-Castro D, Hallgren J. Mast cells contribute to T-cell accumulation in the bronchoalveolar space in mice with IL-33-induced airway inflammation. Immunology. 2024;173(3):590–602. https://doi.org/10.1111/imm.13849

13652567, 2024, 3, Downloaded from https://onlinelibrary.wiley.com/doi/10.1111/imm.13849 by Uppsala University Library, Wiley Online Library on [18/02/2025]. See the Terms and Conditions (https://onlinelibrary.wiley.com/terms-and-conditions) on Wiley Online Library for rules of use; OA articles are governed by the applicable Creative Commons License